

Structural evolutions of spinels under ions irradiations

D. Gosset^{a,*}, D. Simeone^a, M. Dutheil^a, S. Bouffard^b, M. Beauvy^c

^a CEA Saclay, Bat. 453, DMN/SRMA/LA2M, F-91191 Gif/Yvette Cedex, France

^b CIRIL-GANIL, BP 5133, F-14070 CAEN Cedex 5, France

^c DEC, CEA Cadarache, 13108 St Paul-lez-Durance Cedex, France

Available online 1 April 2005

Abstract

Thanks to its high temperature properties and relatively good behaviour under irradiation, the MgAl_2O_4 spinel is considered as a possible material to be used as inert matrix for the minor actinides burning. However, it is known to damage at high fluences. Several studies have shown that the damages induced by irradiation lead first to structural modifications and second to an amorphisation inducing an important swelling. In order to propose a better description of these structural modifications, we have irradiated different spinels at room temperature at Grand Accélérateur National d'Ions Lourds at Caen (GANIL) facility with swift Kr ions. The irradiation damages were characterised by Raman analysis and X-ray diffraction.

Three different materials were irradiated, MgAl_2O_4 and the isomorphic spinels ZnAl_2O_4 and MgCr_2O_4 , this allowing a better X-ray analysis of the cations distributions. Comparing our results with previously published ones, we show that the apparent damage of these materials do not depend on the irradiation conditions. In addition, we have unambiguously observed that the first damage stage is not a phase transformation but an order–disorder transition of the cationic sub-lattice. On the other hand, for the three materials, the cations are distributed on the classical 8a and 16d sites. The inversion rates we derive are however much higher than in non-irradiated materials at high temperatures. But in the Mg-materials, the cations are also located on the normally empty sites 16c and 48f, leading to highly disordered structures.

We have then performed isochronal annealings, which show that the disorder recovers in one stage (ZnAl_2O_4) or in two different stages (MgAl_2O_4 and MgCr_2O_4). The second stage can be attributed to the healing of the cation inversion rate, the first one to the displacement of the cations from the forbidden to the normal positions. In the three cases, the initial structure is totally healed after annealing at 1000 °C. These results could give some clues to explain the amorphisation stage of the spinels under irradiation and help in selecting a better inert matrix material.

© 2005 Elsevier Ltd. All rights reserved.

Keywords: Spinel; Irradiation damage

1. Introduction

In the frame of French nuclear waste management policy, a possible way to reduce the minor actinide (Np, Am, Cm) volume to be stored for long duration is selective burning (i.e. transmutation into short half life elements) in dedicated reactors. This requires the use of ‘neutronically’ inert matrix materials to dilute the actinide to be burned and retain the fission products. Among the possible materials, magnesium aluminate spinel MgAl_2O_4 has been extensively studied,

due to good its chemical inertness, high temperature stability and good neutron irradiation resistance.^{1,2} However, the studies have shown swelling³ of the material and amorphisation at highest fluences. Prior to this amorphisation, drastic structural modifications have been observed and some authors have interpreted them as a crystalline phase transformation.^{4,5} On the other hand, there is no clear evidence for the formation of extended defects such as dislocations loops or networks.⁶

Such an inert matrix will be submitted to irradiation of different origins, namely fast neutrons, α particles (~ 6 MeV) and recoil atoms (~ 240 amu, 100 keV) from natural actinides α -decay, fission products (~ 80 – 150 amu, ~ 70 – 100 MeV).

* Corresponding author. Tel.: +33 1 6908 5857; fax: +33 1 6908 9082.
E-mail address: dominique.gosset@cea.fr (D. Gosset).

These lead to different damage processes, small or large displacement cascades and electronic interactions. Simulating the resulting damage then requires the use of different ion irradiations, light and heavy slow ions and swift heavy ions.

MgAl₂O₄ is part of the spinel family with the general formula AB₂O₄ and *Fd* $\bar{3}m$ space group. Divalent A and trivalent B cations are located respectively on the tetrahedral 8a and octahedral 16d Wyckoff positions, sharing O atoms located on the 32e sites. Due to cationic radii effects, O atoms are slightly shifted from the (1/4, 1/4, 1/4) to a more general (*u*, *u*, *u*) position, leading to octahedral and tetrahedral distortions. Most of the possible cationic sites (16c (octahedral), 8b and 48f (tetrahedral)) are empty. Synthetic materials differ from this ideal scheme and are characterised by a partial inversion of the A and B atoms, mainly depending on the production conditions of the samples. At last, deviations from the theoretical stoichiometry are possible.

In order to improve the understanding of the first damage steps of spinels, we have performed swift heavy ion irradiations in Grand Accélérateur National d'Ions Lourds at Caen (GANIL). The main advantage of such an irradiation is the large nearly homogeneously damaged volume with a thickness around 20–40 μm . We have then performed X-ray analysis of the damaged areas. The major drawback of such an analysis in the case of MgAl₂O₄ spinel is its poor sensitivity to the cation distribution, due to their low atomic mass difference. We have then performed the same investigation on equivalent materials ZnAl₂O₄⁷ and MgCr₂O₄. In addition, we have performed Raman analysis in order to determine the actual local crystal symmetry. In this paper, we confirm that the initial *Fd* $\bar{3}m$ space group is not changed during irradiation,⁸ but the unit cell shows drastic changes with high cationic inversion rates and the occupation of normally empty sites, which depend on the material composition. Moreover, subsequent isochronal annealing show different healing processes in the three materials.

2. Experimental

MgAl₂O₄ powder produced by Bailowsky company containing 1.2% MgO and 0.3% Al₂O₃ was hot-pressed (1 h, 1923 K, 300 MPa under H₂ atmosphere) leading to high density (98% theoretical density), low grain size (3 μm) pellets. High purity ZnO and Al₂O₃ powders were compacted then calcined 1 h at 1473 K and sintered 8 h at 1800 K to produce ZnAl₂O₄ low density (67% theoretical density) pellets⁷. High purity MgO and Cr₂O₃ (Alfa-Aesar) powders were blended and pressed (300 MPa) prior to sintering (1 day at 1200 K) resulting in low density (75%) MgCr₂O₄ pellets. All pellets were then sieved and polished.

X-ray analyses were performed with INEL CPS120 curved position sensitive detectors, before and during ion irradiation at GANIL and after each isochronal annealing. The GANIL facility allows quick spectra collection, but with a poor sensitivity (spectra practically limited to the 20–80° 2θ

range, graphite monochromator selecting Cu K α_{1+2} line). All other spectra (prior and after irradiation and after isochronal annealings) were collected on a second facility with much better optical performance⁹ (parallel Cu K α_1 monochromatic incident beam with low equatorial divergence (Sollers slits), 0–120° 2θ range) and high signal/noise ratio. The refinement of the X-ray diffraction diagrams was performed with the XND Rietveld program.¹⁰

The Raman spectra of irradiated samples were recorded in a back-scattering configuration under a microscope, using a T64000 Jobin-Yvon spectrometer with a CCD detector. A confocal hole was adjusted to enhance the signal coming from the surface. Such a configuration ensures the analysed depth is around 1 μm , much less than the thickness of the damaged zone (cf. infra). To avoid luminescence signal due to impurities, 514.5 and 488 nm excitation laser lines were used.

The irradiations were performed at GANIL with 820 MeV Kr ions at room temperature and a constant flux ($10^9 \text{ cm}^{-2} \text{ s}^{-1}$). The slowing down of the ions (8–12 keV/nm, ranges around 50 μm as estimated with SRIM-2000¹¹) in the zone analysed with X-ray diffraction (thickness around 20 μm) is then due to purely electronic interactions. The contributions of direct displacement cascades can be practically neglected. The fluence ranges from 10^{13} to 10^{15} ions cm^{-2} .

3. Results and interpretation

First, we observed that the diffraction diagrams show the same evolution during the swift ions irradiations than that already observed in quite different irradiation conditions. In Fig. 1, we have reported the diffraction diagrams of MgAl₂O₄ prior and after irradiation. The same modifications as noted by Sickafus et al.^{4,5} are observed. These include the disappearance of all the (*hkl*) apart from the (*4h*, *4k*, *4l*) lines and partial amorphisation for the highest fluences. The same observation can be made when comparing the results obtained by Chukalkin et al. for the irradiation of MgCr₂O₄.¹² However, in the first case the material was irradiated with 400 keV Xe ions at low temperature (20 K) and in the second case, the material was irradiated by neutrons (fast

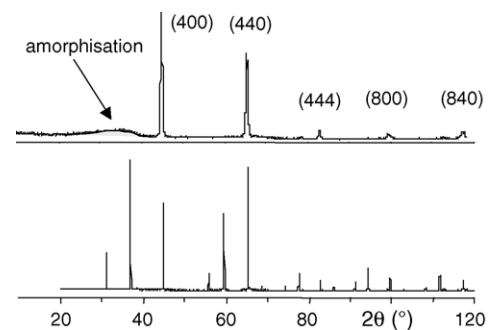


Fig. 1. X-ray diffraction pattern of MgAl₂O₄ prior (bottom) and after (top) ion irradiation. Only the (*4h*, *4k*, *4l*) lines remain.

neutrons $2 \times 10^{20} \text{ cm}^{-2}$, $E > 1 \text{ MeV}$) around 50°C . Finally, irradiations of ZnAl_2O_4 with slow heavy ions show the same evolution of the X-ray diagrams¹³ as observed for the other samples. As a consequence, the (long range) structural modifications induced by irradiation in the spinels we consider do not depend on the initial damage mechanisms, electronic slowing-down and subsequent energy transfer to the structure ions in the case of swift heavy ions, large displacement cascades in the case of slow heavy ions and small displacement cascades in the case of fast neutrons. This result has to be explained and studies are in progress. But it is of primary importance since it allows the comparison of different experiments. Particularly, this validates for these materials the use of ion irradiations as a (cheap) tool to simulate the damages arising from neutron irradiations in reactors or auto-irradiation in long-term storage, with the advantages of an easy control of the experimental parameters (flux, fluence, temperature, electronic versus ballistic damage) and in situ analysis (X-ray diffraction, thermo-mechanical and physical properties).

The second key result is the unambiguous identification of the cell structure of the materials. From TEM observations or X-ray analysis, analogous to the results reported in Fig. 1, many authors assumed that the disappearing of the odd (hkl) lines should be attributed to a cell modification, from $Fd\bar{3}m$ to fcc $Fm\bar{3}m$, together with a cell parameter division by 2. Such a structure can indeed lead to the observed diffraction diagram. To check this point, we have performed Raman analysis on MgAl_2O_4 prior and after irradiation. The result (Fig. 2) clearly shows that the structure is not modified since all the characteristic lines of the $Fd\bar{3}m$ space group remain visible after irradiation. In contrast, the rock salt $Fm\bar{3}m$ space group would show only one line in the same wavelength range.

We have then performed Rietveld analysis of the X-ray diffraction patterns. The results are summarized in Table 1. In the case of ZnAl_2O_4 , all the diagrams could be explained assuming an increase of the classical Zn–Al inversion ratio, with an exponential-like dependence on the fluence. In the case of MgAl_2O_4 , we first tried to simulate the diffraction diagrams assuming again an increase of the inversion ratio. But the atomic diffusion factors of Mg and Al are so close they can hardly be distinguished by X-ray diffraction. Thus, we

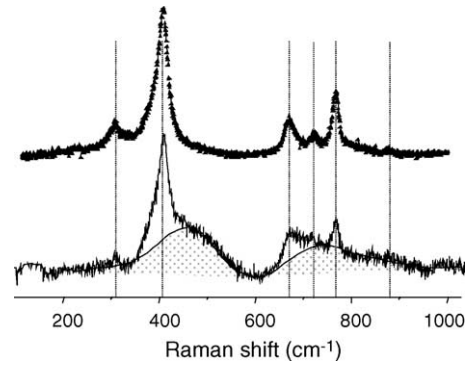


Fig. 2. Raman spectra of non- (top) and irradiated spinel MgAl_2O_4 . Dotted lines: $Fd\bar{3}m$ characteristic lines. Shaded areas: contribution of amorphous material.

Table 2

Relative intensities of (hkl) lines (real and imaginary parts of the structure factor) as a function of the occupancies of the different sites (respectively A for 8a, C for 16c, etc.)

(hkl)	Re	Im
(4 4 0) (8 0 0)	$[8(A+B) + 48F] + [16(C+D)]$	0
(4 0 0) (4 4 4) (8 4 0)	$[8(A+B) + 48F] - [16(C+D)]$	0
(2 2 2) (4 2 2) (6 2 0) (6 4 2)	$8(A+B) - 16F$	0
(2 2 2) (6 2 2) (6 6 2)	0	$-16(C+D)$
(1 1 1) (3 3 1)	$4(A-B) + 4\sqrt{2}(C-D)$	$-\text{Re}$
(3 1 1) (3 3 3)	$4(A-B) - 4\sqrt{2}(C-D)$	Re
(5 1 1)	$4(A-B) - 4\sqrt{2}(C-D)$	$-\text{Re}$
(5 3 1)	$4(A-B) - 4\sqrt{2}(C-D)$	Re

defined a virtual ‘Mg + Al’ atom with a ‘mean’ atomic diffusion factor. This permitted a correct simulation of the XRD pattern of the most irradiated samples.⁸ However, on considering the influence of the occupancy of the different sites on the actual relative intensities of the different (hkl) lines (Table 2) leads us to assume that the cations, beyond the classical inversion, were also partially distributed on normally empty (forbidden) sites (Table 1). In contrast, the oxygen sub-network is little affected. We mainly observe an increase of its Debye–Lorentz coefficient (apparent thermal agitation or poor localisation) and an oxygen atomic position (u) shift lower than 1%. The same structural modifications had also to be assumed to analyse the MgCr_2O_4 XRD patterns. In this

Table 1
Structural modifications of the spinels after 820 MeV Kr irradiation

Site	ZnAl_2O_4				MgAl_2O_4				MgCr_2O_4			
	Initial		Irradiation 7.6×10^{12}		Initial		Irradiation 9.3×10^{12}		Initial		Irradiation 3.8×10^{12}	
	Zn	Al	Zn	Al	Mg	Al	Mg	Al	Mg	Cr	Mg	Cr
8a	0.91	0.09	0.72	0.28	1.00		0.67		1.00		0.44	
8b												
48f							0.25				0.42	
16c							0.09	0.25			0.14	0.67
16d	0.09	1.91	0.28	1.72		1.87		1.62		1.92		1.26
u	0.264		0.262		0.261		0.257		0.260		0.252	
a (Å)	8.081		8.090		8.069		8.066		8.332		8.299	

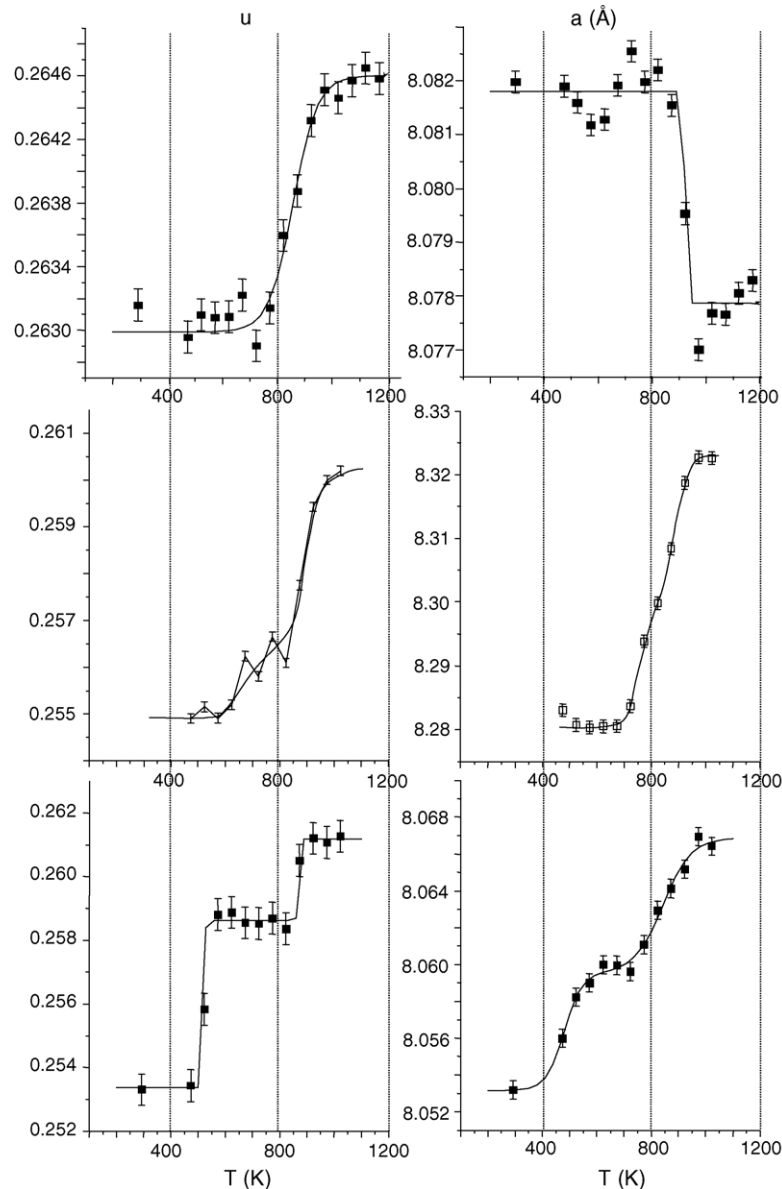


Fig. 3. Isochronal annealings of irradiated spinels vs. annealing temperature (K). Top: ZnAl_2O_4 , middle: MgCr_2O_4 , bottom: MgAl_2O_4 . Left: relative position of 32e site (O), right: cell parameter (\AA).

case, thanks to the cation mass difference, the sensitivity of the analysis is much better and then gives more credence to the approach we adopted for MgAl_2O_4 .

The first question that arises concerns the way the structure can accommodate such modifications. Since the cations can hardly be located on neighbour sites, due to strong Coulombic repulsion, medium-range reorganisation processes must be activated. From re-examination of previously published high-resolution TEM observations,¹⁴ we may assume that reordering of the structure leads to the formation of nano-sized domains with normal inter-site relations (including inversion) separated by partial stacking faults, thus allowing the long-range conservation of the oxygen sub-network we observe. Using X-ray diffraction (long-range analysis) or Raman spectroscopy (local symmetry), such a nanostructured

material could not be differentiated from a homogeneous material with a mixing on 8a, 16c, 16d and 48f sites. HRTEM observations should be performed to check this hypothesis.

In order to improve the description of the irradiation damage, we then performed XRD analysis after isochronal annealings (30 min, 50 °C steps). Preliminary results are summarized in Fig. 3 in which we show the evolution of the most sensitive parameters, i.e. the cell parameter (a) and the relative oxygen position (u). The behaviour of the materials is very different. The material, which has the simplest behaviour, ZnAl_2O_4 , exhibits healing in a single, narrow stage around 850 K. MgAl_2O_4 shows two well-separated stages, around 520 and 870 K and MgCr_2O_4 shows a large stage around 850 K, with a possible first small stage around 720 K. This last result is in good agreement with Chukalkin et al.,¹²

who have shown that the intensities of the diffraction lines of MgCr_2O_4 irradiated with neutrons recover in the same temperature stages, the relative heights of the stages depending on the considered (hkl) 's. From these results, we may assume that in the 'complex' MgAl_2O_4 and MgCr_2O_4 materials, at least two different mechanisms are necessary to heal the structure. The first stage could be attributed to the displacement of the atoms located in the normally forbidden sites to the classical positions. The second stage could allow the recovery of the inversion rates, since it is located in the same temperature range than the classical order–disorder transition in spinels.⁷

4. Conclusion

Different spinel materials have been irradiated with swift heavy ions. The results show that the resulting damage does not depend on the basic irradiation mechanisms. In contrast, Raman spectroscopy shows that the crystal structure is unaffected and remains $Fd\bar{3}m$. However, in the case of MgAl_2O_4 and MgCr_2O_4 , the irradiation leads to the classical cation inversion, as in ZnAl_2O_4 , and also to the occupancy of normally empty sites. At last, isochronal annealings show a more complex behaviour for the two Mg-materials.

Analyses of the diffraction diagrams are in progress. The main questions which now arise are the actual defect structures (occupancy of forbidden sites) in these materials, the scaling of the effects for different impinging particles, the way the global structure accommodates these defects and the parameters controlling the sensitivity of the materials composition. This could help determining a better inert matrix material with improved irradiation resistance.

Acknowledgement

We are very indebted to P. Daniel (LPEC, UPRES A CNRS 6087, F-72085 Le Mans) who performed the Raman analysis.

References

1. Summers, G., White, G., Lee, K. and Crawford, J., *Phys. Rev. B*, 1980, **21**(6), 2578.
2. Sickafus, K. E., Larson, A. C., Yu, N., Nastasi, M., Hollenberg, G. W. and Garner, F. A., *J. Nucl. Mater.*, 1995, **219**(1–3), 128–134.
3. Klaassen, F. C., Schram, R. P. C., Bakker, K., Neeft, E. A. C. and Conrad, R. In *Seventh Information Exchange Meeting on Actinide and Fission Product Partitioning and Transmutation*. Jeju, Republic of Korea, 14–16 October 2002, pp. 549–558.
4. Devanathan, R., Sickafus, K. and Nastasi, M., *Phil. Magn. Lett.*, 1995, **72**(3), 155.
5. Ishimaru, M., Afanassiev-Charkin, I. and Sickafus, K., *Appl. Phys. Lett.*, 2000, **76**(18), 2556.
6. Kinoshita, C., Fukumoto, K., Fukuda, K., Garner, F. and Hollenberg, G., *J. Nucl. Mater.*, 1995, **219**, 143.
7. Dodane-Thiriet, C., Ph.D. thesis 6814, Orsay, Paris-XI University, 2002.
8. Simeone, D., Dodane-Thiriet, C., Gosset, D., Daniel, P. and Beauvy, M., *J. Nucl. Mater.*, 2002, **300**, 151–160.
9. Simeone, D., Gosset, D. and Bechade, J. L., CEA-R 5975 Report, 2001.
10. Berar, J. F. and Baldinozzi, G., *CPD Newslett.*, 1998, **20**, 3.
11. J. Ziegler, <http://www.srim.org/>.
12. Chukalkin, Y., Petrov, V., Shtirts, V. and Goshitskii, B., *Phys. Status Solidi*, 1985, **A92**, 347.
13. Simeone, D., Contribution à l'étude des changements de phases induits par l'irradiation dans des céramiques cristallines isolantes. HDR, Jussieu 2003.
14. Wang, L. M., Wang, S. X., Lian, J., Ewing, R. C. and Arbor, A., In *First Annual Michigan Materials Research Symposium (MMRS)*, 5–6 May 1999.